

Rigidity and connectivity percolation in heterogeneous polymer-fluid networks

David H. Boal

Department of Physics, Simon Fraser University, Burnaby, British Columbia, Canada V5A 1S6

(Received 19 November 1992)

A heterogeneous network which is partially polymerized and partially fluid is studied by Monte Carlo simulation in two dimensions. Within statistical uncertainties, the compression modulus is found to be independent of polymer fraction, while the shear modulus vanishes below the connectivity percolation threshold. This behavior is different from networks without the fluid component, for which the rigidity percolation threshold is roughly double the connectivity percolation threshold.

PACS number(s): 64.60.Ak, 05.40.+j, 68.10.-m, 87.22.Bt

Heterogeneous membranes which are partially fluid and partially polymerized have several experimental realizations. For example, membranes composed of certain phospholipid molecules can be partially polymerized upon exposure to UV light [1–3]. Prior to polymerization, the membrane has a nonzero area compression modulus (K_A) and a vanishing shear modulus (μ) characteristic of a fluid. The fluid behavior of the homogeneous membrane is reduced as the molecules become increasingly polymerized.

A second example comes from red blood cells (RBC's), whose boundary membrane consists of a lipid bilayer attached to an approximately triangular network of spectrin protein [4]. The bilayer is fluid and contributes strongly to the compression modulus. The nonzero shear modulus arises from the spectrin protein network, which has a fixed connectivity on short-time scales [5–7]. Mutant RBC's which are spectrin deficient are found to have a reduced shear modulus compared to normal RBC's [8,9]. These two examples show systems that have fluid connectivity between some elements and fixed connectivity between others.

In this Brief Report we investigate networks containing random polymeric bonds between elements that otherwise have fluid connectivity with their neighbors. It is not clear that either of the examples quoted above in fact have *random* polymerization. For example, in the partially polymerized phospholipid bilayer [1–3], there is indication that the polymerization occurs in patches. However, single-component randomly diluted networks have been investigated in statistical mechanics [10–22] and allow a benchmark against which our randomly polymerized network can be compared.

In randomly diluted networks, bonds or sites are present at random locations with occupation probability p . Above the connectivity percolation threshold p_c a single connected cluster spans the network. Consider first the situation in which the bonds have only stretching resistance, but no bending resistance against neighboring bonds. Then the elastic constants are zero both below and immediately above p_c . It is only at a higher concentration called the rigidity percolation threshold p_R that both elastic constants are nonzero [10]. For a bond-depleted triangular network $p_c = 2 \sin(\pi/18) = 0.35$ and

$p_R \approx \frac{2}{3}$ [11–15]. When bond-bending resistance is introduced, the elastic constants are zero below p_c and nonzero above p_c [16–20]. In studies of the flatness of site [21] and bond [22] diluted membranes embedded in three dimensions, it is found that the membranes are always asymptotically flat for concentrations above p_c .

Random heterogeneous fluid-polymer networks should be different from the single-component random networks since in a heterogeneous network K_A may be always nonzero while only μ vanishes below a critical polymer fraction. In this paper, we determine the two-dimensional elastic constants of a heterogeneous model membrane in which a parameter p represents the degree of polymerization [23].

Our computation is based upon the tethered membrane model [24,25] in which the two-dimensional membrane is represented by a fixed number N of hard spherical beads (or vertices) of diameter a . The beads are linked together by straight flexible tethers, whose maximal length of $\sqrt{3}a$ enforces membrane self-avoidance. In our model, each tether is characterized as either *fluid* or *polymerized*. Fluid tethers, shown in light grey in Fig. 1, can migrate from vertex to vertex subject to computational rules set out below. Polymerized tethers, shown in white in Fig. 1, have fixed connectivity in that their ends are always attached to the same vertices. There is no resistance to in-plane “bending” of the tethers with respect to each other except the resistance associated with the excluded volume of the beads.

A Metropolis Monte Carlo technique is used to generate a set of appropriately weighted sample configurations. A value is chosen for the polymerization fraction p and an initial configuration (which we call a *realization*) at that value of p is generated by randomly labeling each tether as either fluid or polymerized. Because of machine time constraints, we choose to work with only a few realizations of large systems ($N=576$), rather than many realizations of smaller systems. Three realizations are generated at each p simulated above p_c , but only one realization for each p below p_c .

In the simulation, a *sweep* across the membrane involves the following steps: (i) An attempt is made to change the position of each vertex by choosing a new position randomly from within a square box of length $2la$ to

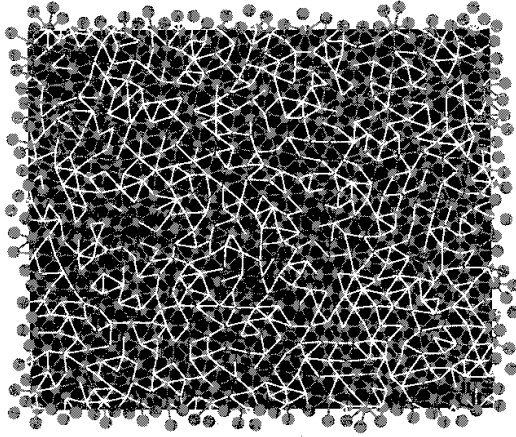


FIG. 1. Sample configuration for polymer fraction $p=0.5$ viewed perpendicular to the plane of the membrane. The fluid tethers are grey, while the polymerized tethers are white.

the side centered on the old position, where we choose $l=0.1$. (ii) An attempt is made to reconnect every fluid tether following the procedure of Baumgartner and Ho [26]. In this procedure, a tether is removed and replaced with a new tether connecting the two “opposite” vertices that (along with the vertices at the ends of the original tether) define the two triangles having the original tether in common. The polymerized tethers are not subject to procedure (ii) since their attachment is permanent. Each trial move is accepted if it does not violate the tether-length and bead-size constraints.

A rectangular membrane “patch” subject to periodic boundary conditions in the x and y directions is used in the simulation. An isobaric simulation is performed by allowing the rectangle lengths L_x and L_y to vary independently. There is one trial move to rescale the rectangle size per sweep. The rescaling moves are accepted with a pseudo-Boltzmann factor [27]

$$W = \exp[-\beta P \Delta A + N \ln(1 + \Delta A / A)], \quad (1)$$

where P is the pressure and ΔA is the difference in the area ($A \equiv L_x L_y$) before and after the rescaling. In these simulations, the pressure has been set to zero.

For each realization, 150 sample configurations are generated. Each configuration is separated by a “Rouse time” $\tau \equiv N/l^2$ Monte Carlo sweeps. Each initialization is allowed to relax for 10τ before sample collection commences. More than 9×10^6 attempted moves are made on each vertex and tether for a given realization. The entire simulation required approximately 7 CPU months on a 33-MHz Model MIPS R3000 processor purchased from Silicon Graphics Inc.

Two independent determinations of Young’s modulus, Y_x and Y_y , are made from fluctuations of the rectangle length in the x and y directions, respectively [28]:

$$\beta Y_x = [\langle A \rangle \langle L_x^2 \rangle / \langle L_x \rangle^2 - 1]^{-1}, \quad (2a)$$

$$\beta Y_y = [\langle A \rangle \langle L_y^2 \rangle / \langle L_y \rangle^2 - 1]^{-1}. \quad (2b)$$

The area compression modulus K_A is determined from the area fluctuations

$$\beta K_A = \langle A \rangle / (\langle A^2 \rangle - \langle A \rangle^2). \quad (3)$$

Finally, the shear modulus μ is obtained from Y and K_A via

$$\mu = Y K_A / (4K_A - Y), \quad (4)$$

where the average of Y_x and Y_y is used for Y in Eq. (4). The equations are used to determine the elastic constants of each realization, and then the results from different realizations at a given polymerization fraction are averaged. With this procedure, our statistical uncertainties are approximately 10%.

The behavior of the elastic constants is shown as a function of polymerized fraction in Fig. 2. The compression modulus $\beta K_A a^2$ is relatively constant within our statistical uncertainties and has a value of 18 ± 1 . By making an analogy with a network of harmonic springs, Kantor and Nelson [25] predict that the polymerized tethered network should have $\beta K_A a^2 \approx 20$, which is close to the value obtained here.

The shear modulus $\beta \mu a^2$ is also shown in Fig. 2. Below $p \approx 0.35$, the shear modulus is zero. Above this fraction, the shear modulus increases roughly linearly towards the pure polymerized membrane value of 9 ± 1 . At $p=1$, we find $K/\mu=2$ within statistical error, as predicted by the harmonic spring model [25]. This linear rise of the shear modulus with p is the same general behavior observed in randomly diluted networks [11–20]. However, for random triangular networks subject only to bond-stretching resistance, the threshold p_R for the appearance of nonzero shear modulus is roughly double the connec-

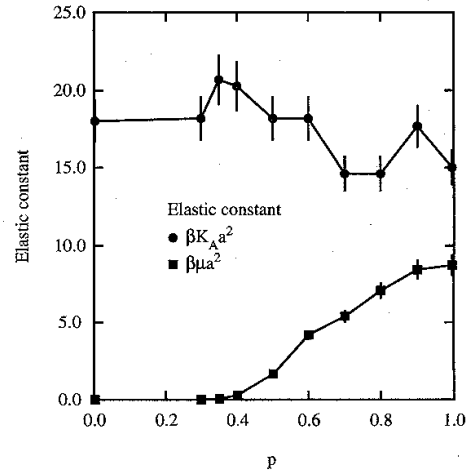


FIG. 2. Compression modulus $\beta K_A a^2$ (circles) and shear modulus $\beta \mu a^2$ (squares) as a function of polymer fraction p . The networks have a total of 576 vertices, and three realizations are performed at each value of p . Estimated uncertainties are approximately 10%.

tivity percolation threshold. For our partially polymerized networks, the two thresholds coincide.

The difference between our network and the randomly diluted networks of Refs. [11–15] can be understood by considering “holes” in the polymerized part of the net. In our network, the holes are filled with vertices connected by *fluid* bonds so the holes have compression resistance. In the bond and site percolation studies, the holes are empty and highly deformable. Hence, our model network should have greater resistance to deformation than the diluted central-force network.

Experimentally, Waugh and Agre [9] find that the effective shear modulus of human RBC's increases linearly with spectrin content, as observed here. However, there are enough difficulties (see Refs. [9,19]) in extracting the true shear modulus near the spectrin percolation threshold from the effective shear modulus measured experimentally, that we are unable to compare our results

with the RBC shear modulus at low spectrin content.

In conclusion, we determine the elastic constants of a heterogeneous network that is partially fluid and partially polymerized. The shear modulus vanishes for polymer fraction p below the connectivity percolation threshold p_c , while above p_c it increases linearly with p . The compression modulus is finite for all p . This behavior is different from bond or site diluted random networks with only bond-stretching resistance, for which p_c is not equal to the rigidity percolation threshold p_R and for which both elastic moduli vanish below p_c .

This work is supported in part by the Natural Sciences and Engineering Research Council of Canada. I thank Evan Evans, David Knowles, Mohandas Narla, Udo Seifert, and Michael Thorpe for stimulating conversations.

-
- [1] E. Sackmann, P. Eggl, C. Fahn, H. Bader, H. Ringsdorf, and M. Schollmeier, *Ber. Bunsenges, Phys. Chem.* **89**, 1198 (1985).
 - [2] H. Ringsdorf, B. Schlarb, and J. Venzmer, *Angew. Chem.* **7**, 113 (1988).
 - [3] M. Mutz, D. Bensimon, and M. J. Brienne, *Phys. Rev. Lett.* **67**, 923 (1991).
 - [4] For a review, see T. L. Steck, in *Cell Shape: Determinants, Regulation and Regulatory Role*, edited by W. Stein and F. Bronner (Academic, New York, 1989), Chap. 8.
 - [5] E. A. Evans and R. Skalak, *Mechanics and Thermodynamics of Biomembranes* (Chemical Rubber, Boca Raton, 1980).
 - [6] T. Stokke, A. Mikkelsen, and A. Elgsaeter, *Eur. Biophys. J.* **13**, 203 (1986); **13**, 219 (1986).
 - [7] D. H. Boal, U. Seifert, and A. Zilker, *Phys. Rev. Lett.* **69**, 3405 (1992).
 - [8] For a review, see J. Palek, *Blood Rev.* **1**, 147 (1987).
 - [9] R. E. Waugh and P. Agre, *J. Clin. Invest.* **81**, 133 (1988).
 - [10] M. F. Thorpe, *J. Non-Cryst. Solids* **57**, 355 (1983).
 - [11] S. Feng and P. N. Sen, *Phys. Rev. Lett.* **52**, 216 (1984).
 - [12] D. J. Bergman and Y. Kantor, *Phys. Rev. Lett.* **53**, 511 (1984).
 - [13] S. Feng, M. F. Thorpe, and E. Garboczi, *Phys. Rev. B* **31**, 276 (1985).
 - [14] M. F. Thorpe and E. Garboczi, *Phys. Rev. B* **35**, 8579 (1987).
 - [15] A. R. Day, R. R. Tremblay, and A.-M. S. Tremblay, *Phys. Rev. Lett.* **56**, 2501 (1986).
 - [16] Y. Kantor and I. Webman, *Phys. Rev. Lett.* **52**, 1891 (1984).
 - [17] S. Feng, P. N. Sen, B. I. Halperin, and C. J. Lobb, *Phys. Rev. B* **30**, 5386 (1984).
 - [18] L. M. Schwartz, S. Feng, M. F. Thorpe, and P. N. Sen, *Phys. Rev. B* **32**, 4607 (1985).
 - [19] M. J. Saxton, *Biophys. J.* **57**, 1167 (1990).
 - [20] The connectivity and rigidity percolation thresholds also coincide for membranes under tension; see W. Tang and M. F. Thorpe, *Phys. Rev. B* **37**, 5539 (1988).
 - [21] G. S. Grest and M. Murat, *J. Phys. (Paris)* **51**, 1415 (1990).
 - [22] M. Plischke and B. Fourcade, *Phys. Rev. A* **43**, 2056 (1991).
 - [23] For related work on lateral diffusion in biomembranes, see M. J. Saxton, *Biophys. J.* **55**, 21 (1989).
 - [24] Y. Kantor, M. Kardar, and D. R. Nelson, *Phys. Rev. Lett.* **57**, 791 (1986).
 - [25] Y. Kantor and D. R. Nelson, *Phys. Rev. A* **36**, 4020 (1987); see also Y. Kantor, *Phys. Rev. A* **39**, 6582 (1989).
 - [26] A. Baumgartner and J.-S. Ho, *Phys. Rev. A* **41**, 5747 (1990).
 - [27] W. W. Wood, *J. Chem. Phys.* **48**, 415 (1968); see also J. P. Hansen and I. R. McDonald, *Theory of Simple Liquids* (Oxford University Press, New York, 1986).
 - [28] Our definitions for the elastic moduli are the same as those in L. D. Landau and E. M. Lifshitz, *Theory of Elasticity* (Pergamon, London, 1959). The calculational techniques for determining the moduli are from Ref. [7].